PAPER

Large-scale, adhesive-free and omnidirectional 3D nanocone anti-reflection films for high performance photovoltaics

ARTICLES

Journal of Semiconductors
(2019) 40, 042601
doi: 10.1088/1674-4926/40/4/042601

Large-scale, adhesive-free and omnidirectional 3D nanocone anti-reflection films for high performance photovoltaics

Lei Tang[1, 2, ‡], Kwong-Hoi Tsui[1, 2, ‡], Siu-Fung Leung[3], Qianpeng Zhang[1, 2], Matthew Kam[1, 2], Hsin-Ping Wang[3], Jr-Hau He[3], and Zhiyong Fan[1, 2, †]

[1]HKUST-Shenzhen Research Institute, Shenzhen 518057, China

[2]Department of Electronic and Computer Engineering, Hong Kong University of Science and Technology (HKUST), Hong Kong, China

[3]Computer, Electrical and Mathematical Sciences and Engineering, King Abdullah University of Science and Technology, Thuwai 23955-6900, Kingdom of Saudi Arabia

Abstract: An effective and low-cost front-side anti-reflection (AR) technique has long been sought to enhance the performance of highly efficient photovoltaic devices due to its capability of maximizing the light absorption in photovoltaic devices. In order to achieve high throughput fabrication of nanostructured flexible and anti-reflection films, large-scale, nano-engineered wafer molds were fabricated in this work. Additionally, to gain in-depth understanding of the optical and electrical performance enhancement with AR films on polycrystalline Si solar cells, both theoretical and experimental studies were performed. Intriguingly, the nanocone structures demonstrated an efficient light trapping effect which reduced the surface reflection of a solar cell by 17.7% and therefore enhanced the overall electric output power of photovoltaic devices by 6% at normal light incidence. Notably, the output power improvement is even more significant at a larger light incident angle which is practically meaningful for daily operation of solar panels. The application of the developed AR films is not only limited to crystalline Si solar cells explored here, but also compatible with any types of photovoltaic technology for performance enhancement.

Key words: antireflection; crystalline Si solar cells; flexible film

Citation: L Tang, K H Tsui, S F Leung, Q P Zhang, M Kam, H P Wang, J H He, and Z Y Fan, Large-scale, adhesive-free and omnidirectional 3D nanocone anti-reflection films for high performance photovoltaics[J]. *J. Semicond.*, 2019, 40(4), 042601. http://doi.org/10.1088/1674-4926/40/4/042601

1. Introduction

Photovoltaic (PV) systems have been widely deployed as a major renewable energy resource in our daily life because they can directly convert solar energy into clean electricity without pollutions. Typically, solar panels are installed outdoors and exposed to all weather conditions, therefore they are normally packaged with protection layers[1, 2]. However, the packaging layer may have a significant reflection of sunlight at the front surface, which leads to the severe dissipation of sun light and output power of solar cells[1, 3, 4]. Therefore, minimizing the front surface reflection of a solar cell is crucial to maximizing device energy conversion efficiency. For instance, commercial solar cell modules are packaged with glass, epoxy and/or ethylene vinyl acetate (EVA), with which the light reflection can reach up to 10%[4–6]. Traditionally, interference AR coating is used to reduce surface reflection[7]. However, this technique is limited by high cost due to the harsh requirement on coating thickness. Unfortunately, the effectiveness of AR coating is light wavelength and incident-angle dependent thus broadband and omnidirectional AR cannot be achieved[7]. Another widely utilized strategy in the photovoltaic industry is texturization of the top surface of packaging[8–10]. Micro-scale texturization helps increase the solar cell absorption through multiple scattering but the surface reflection remains high[11]. Upon the recent development in the nanostructured PV, the fabrication of 3-dimensional (3D) nanostructured AR coatings becomes cost-effective and the coatings have been demonstrated to have broadband light trapping capability[11–17]. The nanostructures provide gradual change in effective refractive index from top to bottom, which distinctly increase light transmittance at the front-side surface. Furthermore, the effectiveness of light trapping remains valid at different light incident angles. However, there are still some drawbacks of this technique including the complicated fabrication processes, relatively poor uniformity and less control of nanostructure geometry[8]. Moreover, nanostructures can be destroyed in an outdoor environment after a long-time usage and the damaged AR layer can lower the performance of solar cell devices[18]. In this case, replaceable AR layers are desirable for the ease of maintenance. As a result, this constitutes an urgent need for a facile, low-cost and scalable technique to fabricate controllable and replaceable nanostructured AR layer for solar cell devices. Previously, we have developed small-scale fabrication of nanostructured AR film with self-cleaning function for high efficiency solar cell devices using porous alumina mold[19]. In this work, to further improve the scalability of the fabrication process, we have developed a wafer scale technique to fabricate large-scale, adhesive-free and omnidirectional 3D nanocone AR films for high performance photovoltaics. Particularly, the flexible AR films are fabricated by replicating in-

Lei Tang and Kwong-Hoi Tsui contributed equally to this work so that they should be the co-first author of this paper.

Correspondence to: Z Y Fan, eezfan@ust.hk

Received 22 JANUARY 2019; Revised 17 MARCH 2019.

verse-nanocone (i-cone) arrays structure mold using polydimethylsiloxane (PDMS), which is a low-cost, highly flexible, UV resistant and optically transparent material. The mold can be reused multiple times without leaving any residue. The AR films can uniformly stick on rigid and flexible solar panels without using adhesive glue. Note that the size of the AR films can be easily scaled up to suit the commercial solar modules by multiple stitching of molds. The effectiveness of the films has been tested on c-Si solar cells packaged with UV-curable epoxy which is used as the packaging materials for solar panels. The reflectance spectra measurements and finite-difference time-domain (FDTD) simulations show that the nanocone structure can significantly reduce the reflectance of the encapsulation layer. The solar cell device with the nanocone AR film demonstrates nearly 10% more daily power output than the device without the AR film. Furthermore, the 3D nanocone AR film shows high-performance with different light incident angles, which is crucial for practical case.

2. Experimental

2.1. Fabrication of i-cone mold

A layer of 5 μm of pure aluminum was sputtered on 4-inches glass wafer using Varian 3180 Sputtering System (SPT-3180). The hexagonal-array nanoindentation with depth of 50 nm and pitch of 1 μm was formed on Al surface through photolithography and dry etching process using ASML Stepper 5000 (PHT-S1) and AST Cirie 200 Etcher (DRY-Metal), respectively. Photoresist AZ7908 was used as the mask in the processes. Afterwards, the inverse-cone (i-cone) array was fabricated using multi-step anodization and wet etching on the Al/Glass wafer on an acidic solution with a proper direct-current (DC) voltages as mentioned in our previous works[19, 20]. A layer of 50 nm Au was finally sputtered onto the surface to prevent any PDMS residue from leaving on the surface during the peel-off process.

2.2. Fabrication of nanocone AR films

A premixed and degassed PDMS (Sylgard 184, Dow Corning 10 : 1 ratio with the curing agent) was directly poured on the Au-coated icone mold. It should be noted that multiple molds can be stitched together as shown in Supplementary Information (Fig. S2(a)) so that an industrial-scale mold can be formed. Afterwards, PDMS was cured at 120 °C for 5 min. Finally, the large-scale PDMS film can be directly peeled off from the mold.

2.3. Device characterization

SEM images were taken by a JEOL JSM-7100F SEM working at 10 kV. UV–Vis spectra of all devices were obtained using home-built ultraviolet/visible measurement setup. The QE measurement of c-Si solar cell devices were carried out by Oriel QE-PV-SI (Newport Corporation). All the *J–V* curves were obtained using solar simulator (Newport Corporation. 91150V) under 1 Sun illumination

3. Results and discussion

In this work, we report a new technique to fabricate a large-scale, adhesive-free and omnidirectional 3-D nanocone anti-reflection films for high performance photovoltaics. The flexible AR films were fabricated by directly replicating inverse-nanocone (i-cone) arrays on the surface of the mold using polydimethylsiloxane (PDMS). It is worth noting that the mold can be reused multiple times without leaving any residue. Moreover, a scalable mold can be achieved by the stitching of molds to achieve different sizes for commercial solar panels. Therefore, the developed approach makes the manufacturing process cost-effective. The effectiveness of the films has been evaluated using polycrystalline Si solar cells. Overall, the light reflectance measurements and finite-difference-time-domain (FDTD) simulations have shown that the 3D nanocone arrays can significantly reduce the surface reflectance of the encapsulation layer and more pronounced improvements have been observed at oblique light incident angles, which are meaningful for practical case. As a result, the nanocone AR films have boosted the daily energy output of the solar cell devices from 0.774 to 0.844 kWh/m^2, which is close to a 10% enhancement over the device without the AR film.

The large-scale AR films were fabricated by directly replicating inverse-nanocone (i-cone) arrays on a 4-inch wafer using polydimethylsiloxane (PDMS) which is a proper material for AR films because of its high UV resistance, flexibility and optical transparency[21]. Figs. 1(a)–1(d) shows the schematics of the nanocone AR film fabrication process. The detailed fabrication process can be found in Experimental Section. In brief, 5 μm of pure aluminium was first sputtered on a 4-inch glass wafer. Thereafter, as illustrated in Figs. 1(a) and 1(b), the aluminium layer was patterned by photolithography and dry etching to form the hexagonal-array nanoindentation with pitch of 1 μm. The pitch can be controlled between 500 nm to 2 μm in photolithography process. Note that the nanoindentation arrays here will initiate the perfect ordered AAO i-cone growth in the subsequent processes[22–25]. After that, i-cone arrays were fabricated by multi-step anodization and pore widening as described in our previous works[19, 20]. Next, 50 nm of gold was sputtered on the i-cone as the antisticking layer. A pre-mixed and degassed PDMS was poured on the mold and heat it on hotplate at 120 °C for 5 min for curing. It should be noted that the thickness of the AR film can be precisely controlled by spin-coating method before curing. As illustrated in Fig. 1(d), the cured PDMS can be directly peeled off from AAO i-cone master. It is worth pointing out that the i-cone master is found to be very durable during the AR film peel-off process and it can be reused for multiple times without leaving any residue. Fig. 1(e) and its inset exhibited the cross-sectional and top views of scanning electron microscopy (SEM) images of i-cone with pitch and height of 1 μm. Obviously, the i-cone array shows perfect ordering and uniformity of thickness which can be attributed to the improved process of fabricating i-cone on wafer instead of ordinary aluminum foil. As a result, the replicated nanocone structures on AR film exhibited excellent control of geometries including height, diameter and ordering in Fig. 1(f).

There are several distinct features in our fabrication process and films making it superior to the existing anti-reflection technologies. Fig. 2(a) shows a 4-inch i-cone mold coated with 50 nm gold. The light diffraction effect on the surface of the mold indicates the excellent regularity of the nanostructures on the top. The size of the mold can be increased from 4 inches to 12 inches or even larger by using a larger glass wafer. Moreover, it is noteworthy that molds can also be scaled up by directly stitching them together as shown in Fig. S1(a) in supporting Information. Therefore, as shown in

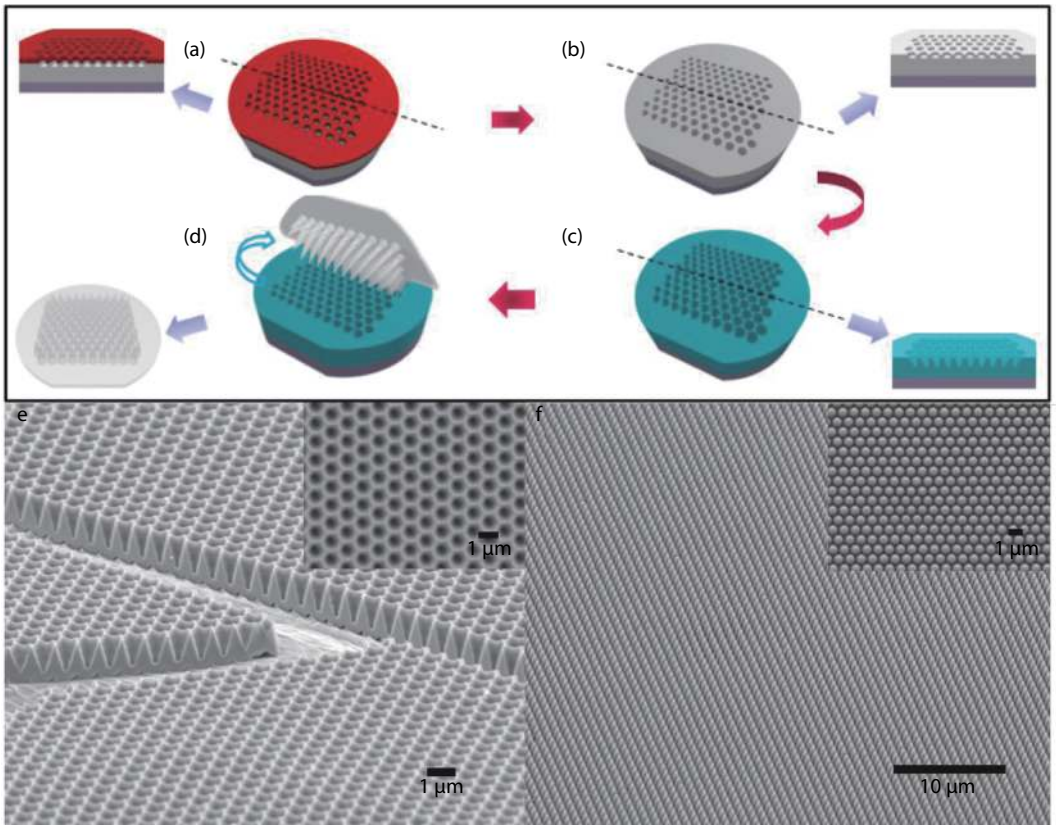

Fig. 1. (Color online) Schematic diagram of fabrication process of i-cone mold and AR film, and SEM images of Au-coated mold and PDMS nanocone. (a) A 4-inch glass wafer with sputtered 5 μm pure aluminum on the surface underwent photolithography of 1 μm hexagonal array pattern. (b) The pattern wafer underwent dry etching to form 50 nm-depth nanoindentation. (c) The wafer underwent anodization to form i-nanocone arrays. (d) The replication and peeloff process of AR film. (e) SEM of Au-coated mold with 1 μm pitch and 1 μm depth. (f) SEM of nanocone with 1 μm pitch and 1 μm depth.

Fig. S1(b), tailored size of films can be made for different sizes of commercial solar panels in the market.

Fig. 2(b) shows the AR film attached to a 180 μm-thick polycarbonate film. Ease of attachment and detachment is one of the appealing features of the nanocone AR film. Traditional AR techniques such as $\lambda/4$ coating and texturization are applied to the surface of solar cells. However, these AR layers are irreplaceable when damaged. Worse still, the damaged layers become a light blocking layer which sacrifices the efficiency of solar cell devices[18]. Owing to the strong Van der Waals attraction between glass/epoxy and PDMS[26], the AR films can be directly attached to and detached from the surface of solar panels without using any glue. As we reported previously, the AR films can possess superhydrophobicity due to synergic effect of nanostructures and hydrophobic properties of PDMS[27, 28]. This property helps to remove light-blocking particles and dust on the surface through the Lotus effect. Fig. 2(c) illustrates the schematic of the device structure after attaching the AR film. It is known that many types of commercial c-Si solar cell modules are encapsulated with glass, EVA or optical epoxy to avoid external shocks and corrosion. Thus, optical epoxy (NOA 81, Norland) was used here as the encapsulation material for the bare c-Si solar cells. As we mentioned before, the AR film can be attached to the surface of the epoxy layer due to the self-adhesion property of PDMS. It is beneficial that additional AR and self-cleaning films can integrate with existing installed solar cell modules without the need for complicated processing. Fig. 2(d) shows a c-Si device, which is 8 cm by 8 cm in size, was covered by the AR film. The details of fabrication process of c-Si solar cell can be found in our previous works[29]. From the cross-sectional and top views of SEM images in Figs. S2(a)–S2(b) in supporting Information, there are random micropyramid structures on the surface of the c-Si solar cells for antireflection function[4, 29]. However, the structures will be covered subsequently by encapsulation materials so that no antireflection effect can be done for incoming light at the air-epoxy interface.

Optical reflectance spectra with wavelength from 400 to 900 nm are shown in Fig. 3(a) in order to quantitatively study the antireflection performance of the AR films. c-Si devices with and without attaching the AR film were placed at the normal direction to the light beam inside an integrated sphere of a home-built ultraviolet/visible measurement setup. The optical reflectance spectrum of an epoxy-encapsulated sample was also measured to evaluate the effect of encapsulated materials on bare c-Si solar cell devices and verify the enhancement effect of AR films on commercial packaged solar cell devices. In the entire visible light region, the AR film-attached c-Si device showed apparently lower reflectance compared to the bare and epoxy-encapsulated c-Si devices. The integrated reflectance of the AR film-attached c-Si device was suppressed to 4.62% while that of the bare and epoxyencapsulated c-Si device were 5.62% and 6.24% respectively. In other words, the AR film reduced light reflectance by 17.7% and 26.0% when respectively compared to the bare and epoxyencapsulated c-Si device, respectively. The reduction of reflectance is mainly due

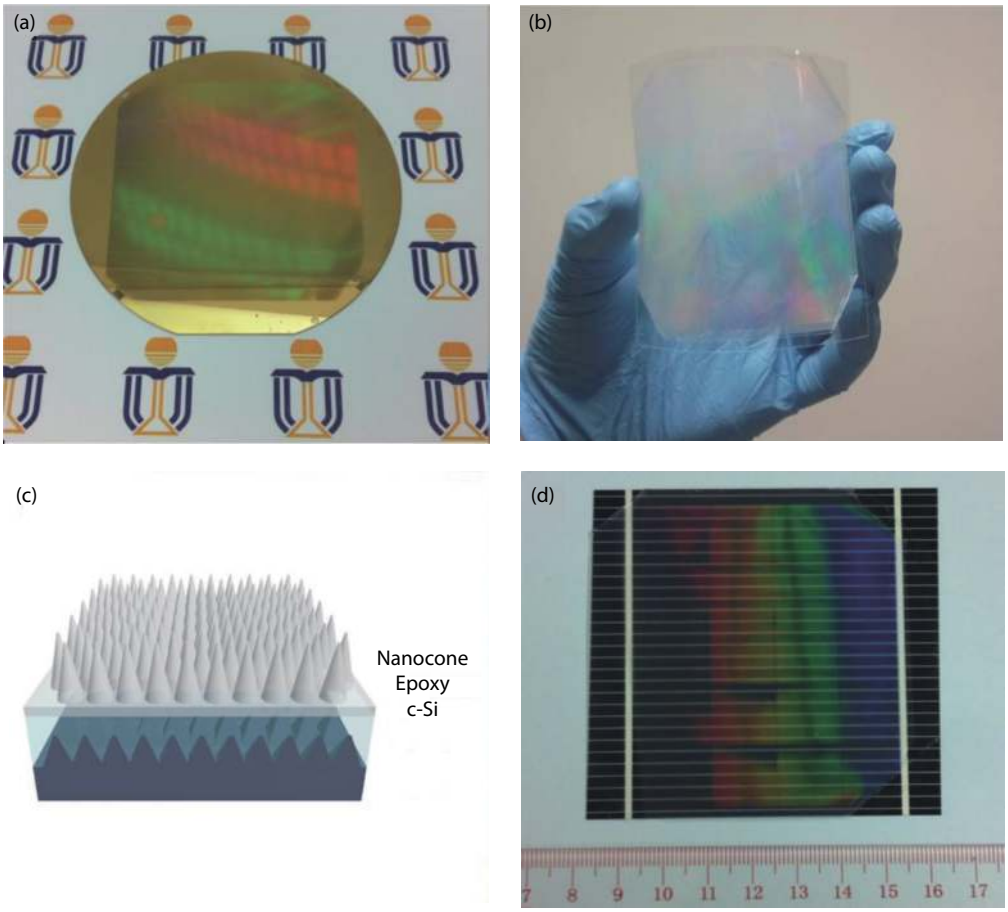

Fig. 2. (Color online) (a) The photograph of 4-inch Au-coated mold. (b) The photograph of flexible AR film attached on polycarbonate film. (c) Schematic diagram of the c-Si solar cell device with nanocone AR film attached on the top. (d) Real 8 cm by 8 cm AR film attached on c-Si device.

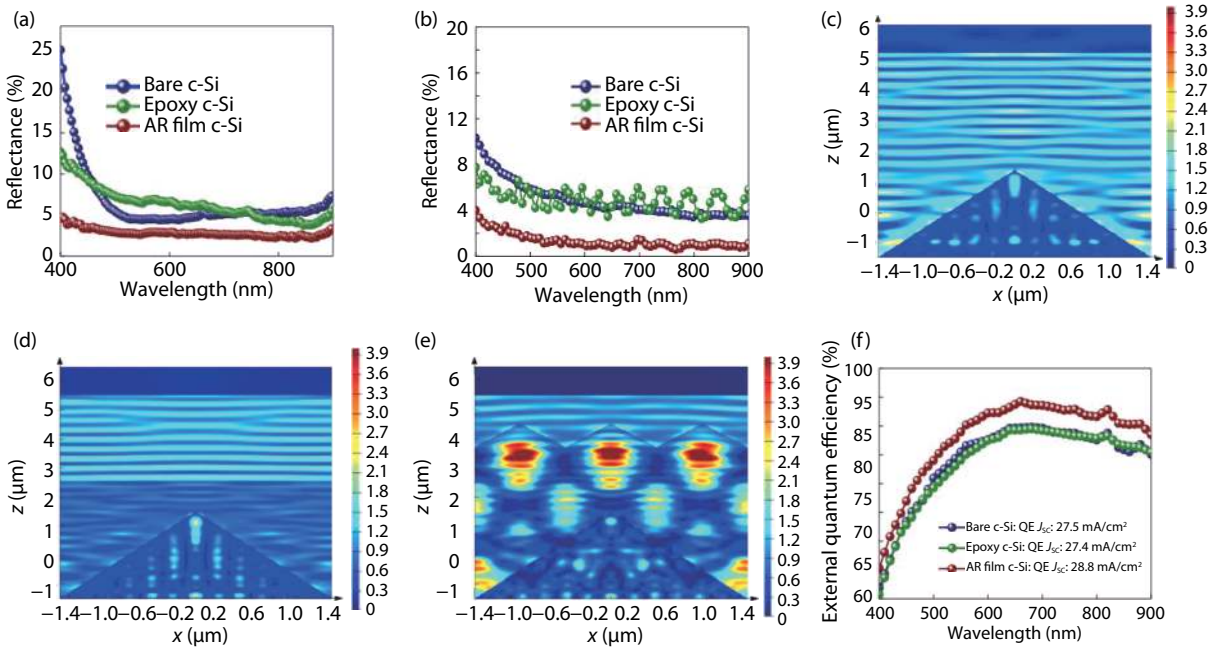

Fig. 3. (Color online) (a) The reflectance spectra of c-Si solar cell device with and without epoxy layer and nanocone AR film in optical wavelength from 400 to 900 nm. (b) Simulations of reflectance spectra in optical wavelength from 400 to 900 nm of c-Si solar cell device with and without epoxy layer and nanocone AR film. (c) Simulated $|E|^2$ distribution of electromagnetic wave at 650 nm wavelength for the bare c-Si device. (d) Simulated $|E|^2$ distribution of electromagnetic wave at 650 nm wavelength for the epoxy-encapsulated c-Si device. (e) Simulated $|E|^2$ distribution of electromagnetic wave at 650 nm wavelength for the AR film-attached c-Si device. (f) QE measurement of c-Si solar cell device with and without epoxy layer and nanocone AR film.

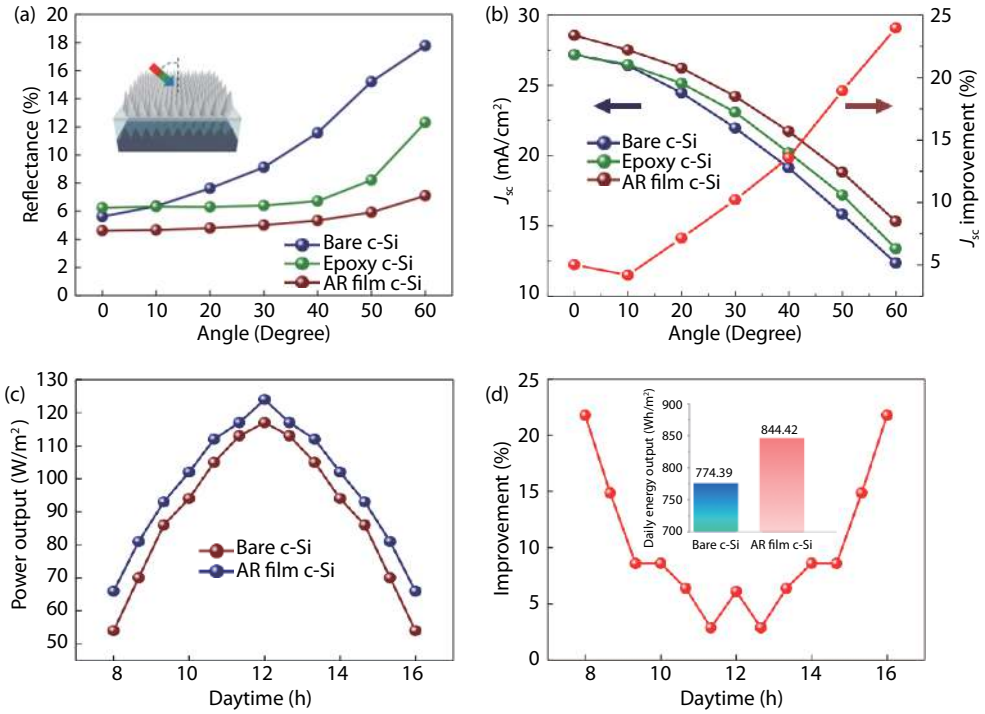

Fig. 4. (Color online) (a) Reflectance spectra of a c-Si solar cell device with and without epoxy layer and AR film obtained for the light incident angles tuning from 0° (normal incident) to 60° at 10° intervals. (b) J_{sc} of a c-Si device with and without epoxy layer and AR film obtained at different incident angles, together with the angular-dependent relative improvement of J_{sc}. (c) Power output of a c-Si device with and without epoxy layer and AR film against daytime. (d) Power output improvement of a c-Si device with and without epoxy layer and nanostructure AR film against daytime, with their daily energy output in the inset.

to the tapered nanocone shape, which provides a gradual change of effective refractive index[30, 31]. However, a few percent of reflectance is remained after using the AR film, which originates from the reflectance from the underneath layers including epoxy and c-Si device. It is interesting that the epoxy-encapsulated c-Si device showed lower reflectance at near UV region (< 460 nm) compared to the bare c-Si device. It can be explained by the Fresnel's equation that the large difference in refractive index happening at air (n = 1.0003 at λ = 460 nm) and c-Si device (n = 4.5766 at λ = 460 nm) interface causes severe light reflection. Furthermore, microscale surface texturization at c-Si surface is less effective in trapping light at this region. On the other hand, epoxy exhibiting much lower refractive index (n = 1.56 at λ = 460 nm) provides an intermediate layer between the c-Si and air. Therefore, a high reflectance at near UV range was obtained in the bare c-Si device. This phenomenon was further verified in the FDTD simulation.

To verify the reflectance spectra obtained from the experiments, optical simulation were performed using FDTD method with results shown in Fig. 3(b). In the FDTD simulation of reflectance spectra, the overall trend for those three devices is consistent with the result obtained from experiments. The AR film showed an excellent reduction in light reflection for the visible light region. On the contrary, both the bare Si and epoxy-encapsulated device showed higher reflection than with AR film. This means epoxy itself cannot reduce the light reflection and the nanostructure plays a key role for AR. In order to understand the AR mechanism in nanostructures, more specifically the nanocones, the cross-sectional electric field intensity ($|E|^2$) distribution were studied and the results are shown in Figs. 3(c)–3(e). Noting that electromagnetic (EM) plane waves propagate downwards from z = 5.5 μm. A c-Si pyramid arrays was used to imitate the surface roughness of c-Si device. Epoxy thin film and nanocones were added to the devices in Figs. 3(d) and 3(e) respectively. The base of a c-Si pyramid, the top surface of epoxy and the top of the nanocone locate at z = −1.5, 2.5 and 4.5 μm respectively more importantly, the color above z = 5.5 μm manifests the intensity of the reflected wave. It can be seen that the existence of nanocone results in the weakest intensity of the reflected wave among these three models, which clearly demonstrates the AR effect of nanocones. The reason for the AR effect is that the nanocones, working as focusing lens, strongly couples the light into the device, as can be clearly seen in Fig. 3(e).

The main function of AR layer is to reduce the optical reflectance on solar cells so that more incoming photons can be utilized and, eventually, the device performance can be enhanced. Therefore, the external quantum efficiency (EQE) measurement was conducted for those three devices. From the result, the EQE curve of the AR film-attached c-Si device is obviously higher than others. It provides a direct evidence of the AR effect. Notably, the EQE at 650 nm reaches almost 95% which is extraordinarily high in c-Si devices. Regarding the EQE current density (QE J_{sc}), the QE J_{sc} of c-Si device after using the AR film was increased from 27.5 to 28.8 mA/cm^2, which indicated around a 4% enhancement. Research has shown that it is challenging for high-efficiency solar cells to have a marginal improvement. In the industry, enhancing the device performance may involve re-designing device structures which may lead to a high capital investment. Introducing an additional AR film on the top of the device can make industrial process cheaper and easier.

Since the incident angle of the sunlight changes with daytime, the angular-dependent performances, both optical and electrical, have been evaluated for light incident angles from 0° to 60°. Fig. 4(a) shows the angular-dependent reflectance of different devices, it is obvious that the reflectance of the AR film-attached c-Si device remains around 4%–6% when the light incident angle increases from 0° to 60°. However, the bare c-Si device reflectance increases from 5% to 18% when the light incident angle changes from 0° to 60°. Therefore, after using the nanocone AR film, a 17.9% to 60% reduction of reflectance can be achieved when the light incident angle increases. As reported in the previous work, this result can be attributed to the angular AR effect which shows more pronounced light scattering effect at a larger light incident angle. As a result, the AR films have an omnidirectional anti-reflection function for solar cell devices. To examine the enhancement in the electrical output, the angular-dependent electrical performance was evaluated by solar simulator under 1 Sun illumination. The result is shown in Table S1 in the Supporting Information. Short-circuit current density (J_{sc}) is the major parameter that can reflect the effect of increasing light absorption because it reflects the capability of incoming photons to convert to electrons. Fig. 4(b) shows that angular J_{sc} of different devices. When comparing the J_{sc} of the AR film-attached device with that of the bare device from 0° to 60°, the enhancement in the angular J_{sc} is from 1.3 mA/cm^2 to 3.0 mA/cm^2. Nevertheless, the relative improvement of J_{sc} progressively increases from 5% to 24% when the incident angle increases from 0° to 60°. To further evaluate this point, output power of the device is plotted against daytime assuming normal incidence which corresponds to noon time, and 60° which corresponds to 4 h away from noon time. As shown in Fig. 4(c), the AR film-attached c-Si solar device demonstrates an all-day improvement of electrical output power, with the percentage improvement showed in Fig. 4(d). With these results, daily energy output can be readily calculated and is shown in the inset of Fig. 4(d) and Table S2. Interestingly, the solar cell device with the AR film demonstrates 0.844 kWh/m^2 daily energy output, which is more than 10% enhancement over the bare sample. Therefore, it is clearly shown that the antireflection effect of the AR films are omnidirectional and are useful in practical operation of solar cell devices.

4. Conclusion

In conclusion, we have demonstrated large-scale, flexible, adhesivefree and omnidirectional 3-D nanocone anti-reflection films for high efficiency photovoltaics. The scalable AR film fabrication process enables a promising and cost-effective technique for a new generation of antireflection technology. From our optical and electrical measurement results, the c-Si solar cell with the AR film shows an excellent broadband suppression of surface light reflectance by 17.7%, which leads to a 6% improvement in device efficiency when light comes from the normal direction. Furthermore, the enhancement is more pronounced at a larger light incident angle which attains 13.3% of the efficiency improvement at 60°. As a result, more than 10% of electricity is generated in a day after using the AR films. The technology reported here can certainly benefit the PV industry and wide adoption of clean solar energy harvesting.

Acknowledgements

This work was supported by National Natural Science Foundation of China (Project No. 51672231), Shen Zhen Science and Technology Innovation Commission (Project No. JCYJ20170818114107730) and Hong Kong Research Grant Council (General Research Fund Project Nos. 16237816, 16309018). The authors also acknowledge the support from the Center for 1D/2D Quantum Materials and the State Key Laboratory on Advanced Displays and Optoelectronics at HKUST.

References

[1] Klampaftis E, Richards B S. Improvement in multi-crystalline silicon solar cell efficiency via addition of luminescent material to EVA encapsulation layer. Prog Photovoltaics Res Appl, 2011, 19, 345

[2] Pern F J, Glick D H, Czanderna A W. Review of the photothermal stability of EVA pottants: effects of formulation on the discoloration rate and mitigation methods. AIP Conference Proceedings, 1996, 353, 1

[3] Miller D C, Muller M T, Kempe M D, et al. Durability of polymeric encapsulation materials for concentrating photovoltaic systems. Prog Photovoltaics Res Appl, 2013, 21, 631

[4] Ramrakhiani M. Recent advances in photovoltaics. Millersville, PA: Materials Research Forum, 2017

[5] Chen J, Zhou L, Ou Q, et al. Enhanced light harvesting in organic solar cells featuring a biomimetic active layer and a self-cleaning antireflective coating. Adv Energy Mater, 2014, 4, 1301777

[6] Eisele C, Nebel C E, Stutzmann M. Periodic light coupler gratings in amorphous thin film solar cells. J Appl Phys, 2001, 89, 7722

[7] Nelson J. The physics of solar cells. London: Imperial College Press, 2003

[8] Gwon H, Park Y, Moon C, et al. Superhydrophobic and antireflective nanograss-coated glass for high performance solar cells. Nano Res, 2014, 7, 670

[9] Deubener J, Helsch G, Moiseev A, et al. Glasses for solar energy conversion systems. J Eur Ceram Soc, 2009, 29, 1203

[10] Li X, He J, Liu W. Broadband anti-reflective and water-repellent coatings on glass substrates for self-cleaning photovoltaic cells. Mater Res Bull, 2013, 48, 2522

[11] Wang H, Periyanagounder D, Li A, et al. Fabrication of silicon hierarchical structures for solar cell applications. IEEE Access, 2019, 7, 19395

[12] Lim S, Um D, Ha M, et al. Broadband omnidirectional light detection in flexible and hierarchical ZnO/Si heterojunction photodiodes. Nano Res, 2017, 10, 22

[13] Tavakoli M M, Lin Q, Leung S, et al. Efficient, flexible and mechanically robust perovskite solar cells on inverted nanocone plastic substrates. Nanoscale, 2016, 8, 4276

[14] Zheng X, Wei Z, Chen H, et al. Designing nanobowl arrays of mesoporous TiO_2 as an alternative electron transporting layer for carbon cathode-based perovskite solar cells. Nanoscale, 2016, 8, 6393

[15] Fan Z, Ruebusch D, Rathore A, et al. Challenges and prospects of nanopillar-based solar cells. Nano Res, 2009, 2, 829

[16] Yu M, Long Y, Sun B, et al. Recent advances in solar cells based on one-dimensional nanostructure arrays. Nanoscale, 2012, 4, 9

[17] Das S, Hossain M J, Leung S, et al. A leaf-inspired photon management scheme using optically tuned bilayer nanoparticles for ultra-thin and highly efficient photovoltaic devices. Nano Energy,

2019, 58, 47

[18] Jiang S, Wang K, Zhang H, et al. Encapsulation of PV modules using ethylene vinyl acetate copolymer as the encapsulant. Macromol React Eng, 2015, 9, 5

[19] Tsui K H, Lin Q, Chou H, et al. Low-cost, flexible and self-cleaning three-dimensional anti-reflection nanocone arrays for high efficiency photovoltaics. Adv Mater, 2014, 26, 2805

[20] Lin Q, Leung S, Tsui K, et al. Programmable nanoengineering templates for fabrication of three-dimensional nanophotonic structures. Nanoscale Res Lett, 2013, 8, 1

[21] McIntosh K R, Powell N E, Norris A W, et al. The effect of damp-heat and UV aging tests on the optical properties of silicone and EVA encapsulants. Prog Photovoltaics Res Appl, 2011, 19, 294

[22] Qiu Y, Leung S, Zhang Q, et al. Efficient photoelectrochemical water splitting with ultrathin films of hematite on three-dimensional nanophotonic structures. Nano Lett, 2014, 14, 2123

[23] Leung S F, Gu L, Zhang Q, et al. Roll-to-roll fabrication of large scale and regular arrays of three-dimensional nanospikes for high efficiency and flexible photovoltaics. Sci Rep, 2014, 4

[24] Leung S, Yu M, Lin Q, et al. Efficient photon capturing with ordered three-dimensional nanowell arrays. Nano Lett, 2012, 12, 3682

[25] Choi J, Wehrspohn R B, Gösele U. Moiré pattern formation on porous alumina arrays using nanoimprint lithography. Adv Mater, 2003, 15, 1531

[26] Galliano A, Bistac S, Schultz J. Adhesion and friction of PDMS networks: molecular weight effects. J Colloid Interface Sci, 2003, 265, 372

[27] Crawford R J, Ivanova E P. Superhydrophobic surfaces. Amsterdam, Netherlands: Elsevier, 2015

[28] Tsui K, Li X, Tsoi J K H, et al. Low-cost, flexible, disinfectant-free and regular-array three-dimensional nanopyramid antibacterial films for clinical applications. Nanoscale, 2018, 10, 10436

[29] Tsai M, Tu W, Tang L, et al. Efficiency enhancement of silicon heterojunction solar cells via photon management using graphene quantum dot as downconverters. Nano Lett, 2016, 16, 309

[30] Lin Y, Lai K Y, Wang H, et al. Slope-tunable sinanorod arrays with enhanced antireflection and self-cleaning properties. Nanoscale, 2010, 2, 2765

[31] Cai J, Qi L. Recent advances in antireflective surfaces based on nanostructure arrays. Mater Horiz, 2014, 2, 37